



Synthesis and Characterization of Thermotropic Liquid Crystals Consisting Heterocyclic Benzothiazole Core System

KOK-LEEI FOO¹, SIE-TIONG HA^{1,*} and SIEW-LING LEE²

¹Department of Chemical Science, Faculty of Science, Universiti Tunku Abdul Rahman, Jln Universiti, Bandar Barat, 31900 Kampar, Perak, Malaysia

²Ibnu Sina Institute for Fundamental Science Studies, Universiti Teknologi Malaysia, 81310 UTM Skudai, Johor, Malaysia

*Corresponding author: Email: hast_utar@yahoo.com

Received: 28 January 2014;

Accepted: 21 March 2014;

Published online: 6 November 2014;

AJC-16198

A new series of rod-shaped mesomorphic compounds, 6-methyl-2-(4-alkoxybenzylidenamino)benzothiazoles bearing a fused thiazole ring and imine central linkage, were prepared and their molecular structures were confirmed *via* mass spectrometric, IR and NMR spectroscopic techniques. The mesomorphic properties were identified using differential scanning calorimetry, polarizing optical microscopy and X-ray diffraction analysis. All compounds showed enantiotropic mesomorphism. Whilst the lower members of the series, butyloxy, hexyloxy and octyloxy derivatives exhibited nematic phase, the medium members (decyloxy derivative) exhibited nematic and smectic A phases. The higher members (C12, C14, C16 and C18 derivatives) displayed smectic A phase only.

Keywords: Imine, Benzothiazole, Mesomorphic, Nematic, Smectic.

INTRODUCTION

At the present day, liquid crystals have turned out to be the basic molecular electronic materials that are used in our daily life. These materials have useful applications in the field of surfactant and detergents, high yield strength polymers, membrane, photonic, thin films, semi-conductors *etc.*¹. Interest in mesomorphic heterocyclic compounds has dramatically increased in recent years due to their larger range of structural templates, as well as their optical and photochemical properties².

Ability to generate lateral and/or longitudinal dipoles is among the great significance of heterocycles as core units in thermotropic liquid crystal. The introduction of heterocyclic fragment is always accompanied with changes in the molecular shape³. These structures basically incorporated unsaturated atoms, such as, oxygen, nitrogen, sulfur and/or others and the presence of such electronegativity atoms often yielded in a reduced symmetry for the overall molecules and a stronger polar induction². The heterocyclic compounds involved are usually five- or six- membered and they form part of the central core in a typical rod-shaped molecule. In previous studies, benzothiazole ring was incorporated as a mesogenic core in thermotropic liquid crystals which allowed them to display good mesomorphic properties⁴. Prajapati and Bonde have synthesized two series of mesogenic benzothiazole derivatives with polar nitro substituent. It was found that the molecular

elongation by addition of phenyl ring and a central ester linkage generated higher mesophase thermal stability. The nitro substituent is also more conducive to the generation of smectic mesophase as compared to the chloro and the methoxy substituent⁵. The substitution at the sixth position was thermally more stable compared to fifth position of benzothiazole ring⁶. In this paper, we reported the mesomorphic properties of heterocyclic benzothiazole liquid crystal with a homologous series of Schiff base ether, 6-methyl-2-(4-alkoxybenzylidenamino)-benzothiazoles⁷. The present study represents an expansion of our existing works in this area^{4,8,9}.

EXPERIMENTAL

All solvents and reagents were obtained commercially and used without any further purification. 4-Hydroxybenzaldehyde, potassium carbonate and 1-bromoalkanes were obtained from Merck (Darmstadt, Germany). 2-Amino-6-methylbenzothiazole was purchased from Acros Organics (USA).

Infrared spectroscopy was performed on a Perkin-Elmer System 2000 FTIR spectrometer. ¹H NMR (400 MHz) and ¹³C NMR (100 MHz) spectra were recorded in CDCl₃ using a Bruker Avance 400 MHz Spectrometer. EI-MS (70 eV) spectrum was collected with a mass spectrometer Finnigan MAT 95XL-T.

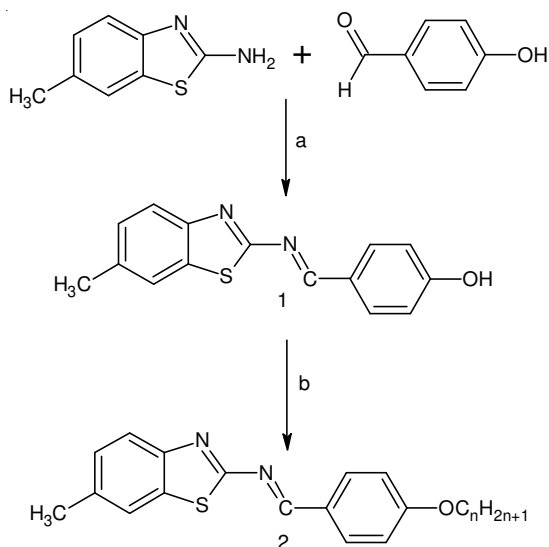
Phase transition temperatures and enthalpy changes were obtained using Mettler Toledo DSC823e at heating and cooling rates of 10 °C min⁻¹. Carl Zeiss polarizing optical microscope

(POM) equipped with Linkam hotstage was used for temperature-dependent studies of the textures of liquid crystals. Textures exhibited by the compounds were observed using polarized light with crossed polarisers. Samples were prepared as thin films sandwiched between a glass slide and cover slip. Mesophase identification was done by comparing the observed textures with those reported in the literature^{10,11}.

Synchrotron powder X-ray diffraction measurements were carried out using beamline B117A at the National Synchrotron Radiation Research Center in Taiwan, where the X-ray wavelength used was 1,32633Å. The XRD data were obtained using imaging plates (area = 20 cm × 40 cm with a pixel resolution of 100) curved with a radius equivalent to a sample-to-image plate distance of 280 mm and the diffraction signals were accumulated for 3 min the powder samples were packed into capillary tube and heated by a heat gun, where the temperature controller was programmed by a PC with a PID feedback system. The scattering angle θ was calibrated by a mixture of silver behenate and silicon.

Synthesis of benzothiazole 1: Equimolar of 2-amino-6-methylbenzothiazole (40 mmol, 6.56 g) and 4-hydroxybenzaldehyde (40 mmol, 4.88 g) were refluxed for 3 h in an ethanol solution (60 mL) with the addition of acetic acid (two drops) as catalyst. The reaction mixture was then filtered and the filtrate was left to evaporate in the fume hood. The yellow solid thus obtained was recrystallized from ethanol before being used for further reaction (**Scheme-I**).

Synthesis of benzothiazole 2: Benzothiazole 1 (20 mmol, 5.8 g) dissolved in minimum amount of N,N'-dimethylformamide is etherified with the suitable 1-bromoalkanes. Anhydrous potassium carbonate is added into the mixture. The mixture was then heated at 80 °C for 5 h. Finally, the precipitate formed upon cooling was filtered off and the solvent was removed by slow evaporation. The yellow product was recrystallized several times with ethanol where upon the pure compound was obtained. The purity of all compounds was checked by thin layer chromatography (Merck 60 F 254) and visualised under shortwave UV light.



Scheme-I: Reagents and reaction condition: (a) C₂H₅OH, CH₃COOH, reflux for 3 h; (b) (CH₃)₂CO, DMF, K₂CO₃, C_nH_{2n+1}Br (where n = 4, 6, 8, 10, 12, 14, 16, 18), reflux for 3 h

The IR, NMR (¹H and ¹³C) and mass spectral data for the representative compound, 12MeBTH, are summarized as follow. Yield 65 %; EI-MS *m/z* (rel. int. %): 283 (38.8) [M⁺], 452 (100); IR (KBr, ν_{\max} , cm⁻¹): 1286 (C-O aromatic ether), 1567 (C=N thiazole), 1597 (C=N Schiff base), 2919, 2849 (C-H aliphatic), 3053 (C-H aromatic); ¹H NMR (400 MHz, CDCl₃): δ 0.90 (t, 3H, *J* = 6.9 Hz, CH₃-), 1.27-1.49 (m, 18H, CH₂-), 1.80 (p, 2H, *J* = 6.9 Hz, -CH₂-CH₂-O-), 2.48 (s, 3H, CH₃-), 4.03 (t, 2H, *J* = 6.6 Hz, -CH₂-O-Ar-), 6.99 (d, 2H, *J* = 8.7 Hz, Ar-H), 7.27 (d, 1H, *J* = 8.1 Hz), 7.61 (s, 1H, Ar-H), 7.83 (d, 1H, *J* = 8.1 Hz, Ar-H), 7.96 (d, 2H, *J* = 8.7 Hz, Ar-H), 8.94 (s, 1H -N=CH-). ¹³C NMR (100 MHz, CDCl₃): δ 164.93 (CH=N), 163.51, 149.84, 134.97, 134.49, 132.24, 127.84, 127.56, 122.40, 121.42, 114.99 for Ar-C, 68.39 (Ar-O-CH₂-), 31.92 (Ar-O-CH₂-CH₂-), 29.65, 29.63, 29.58, 29.55, 29.35, 29.11, 25.98, 22.68, 21.56 [CH₃(CH₂)₉-O], 14.10 (-CH₂CH₃).

RESULTS AND DISCUSSION

The synthetic route towards the targeted compounds is shown in **Scheme-I**. Molecular structure of nMeBTH is confirmed using mass spectrometric, infrared and nuclear magnetic resonance spectroscopic techniques. The predominant molecular ion peak at 452.3 *m/z* in the mass spectrum of 12MeBTH establish its molecular formula as C₂₇H₃₅N₂OS, supporting the proposed structure.

FT-IR spectra of all the members in the series showed the similar characteristics, thus, 12MeBTH is discussed as a representative case. The diagnostic absorption band resulting from the alkyl groups were observed between 2849 and 2916 cm⁻¹. The relative intensity of the absorption bands of the alkyl groups increased upon ascending the series due to increasing number of carbons in the alkyl chain. The absorption band of azomethine (C=N) group was overlapping with the absorption band arising from the C=N stretch of the benzothiazole ring, hence, resulting in a sharp and strong absorption bands at 1597 cm⁻¹. Moreover, a strong band can be observed at 1286 cm⁻¹ which attributed to the C-O ether bond.

According to ¹H NMR spectrum of 12MeBTH, the triplet at δ = 0.90 ppm in the spectra is assigned to the terminal methyl protons. The multiplet signal at δ = 1.27-1.49 ppm, pentet at δ = 1.80 ppm and a triplet at δ = 4.03 ppm were attributed to the remaining methylene protons of the alkoxy chain. A singlet signal at δ = 2.48 ppm is attributed to the methyl protons that directly attached to aromatic ring. The spectrum confirmed the presence of seven aromatic protons. The singlet arising from the azomethine proton was detected at δ = 8.94 ppm^{12,13}. In the ¹³C NMR spectra, the peak at δ = 164.93 ppm is assigned to the azomethine carbon^{12,13}. The signals between δ = 114.99 to 163.51 ppm supported the presence of aromatic carbons whereas the carbons resonances appeared between δ = 14.10 to 31.92 ppm were indicative of the methylene and methyl carbons of the alkoxy chain. The results from the IR and NMR spectral data of the title compounds were consistent with the proposed structure.

The mesophases of all compounds were observed under a POM during heating and cooling cycles. All the compounds exhibited mesomorphism. The phase transition temperatures and corresponding enthalpy changes of compounds nMeBTH were determined using a DSC. The data obtained from the

DSC analysis are summarized in Table-1. The DSC thermograms of 8MeBTH and 10MeBTH during heating and cooling scans are depicted in Figs. 1 and 2, respectively. 8MeBTH exhibited monotropic smectic A (SmA) phase whereby the SmA phase can be observed during cooling cycle only. The existence of SmA phase regardless during heating or cooling processes and thus, it is confirmed that 10MeBTH possessed enantiotropic SmA phase. Both thermograms also showed enantiotropic nematic properties.

On cooling the isotropic liquid of whole series, C4, C6, C8 and C10 members showed droplets which coalesce to a

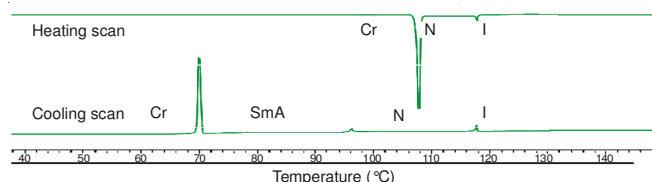


Fig. 1. Differential scanning calorimetry thermogram of 8MeBTH during heating and cooling scans

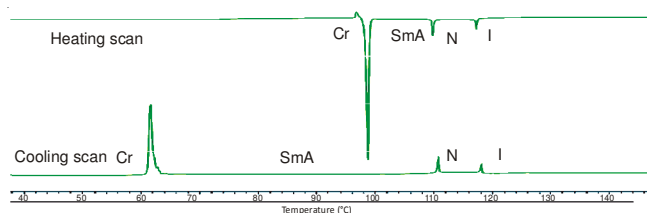


Fig. 2. Differential scanning calorimetry thermogram of 10MeBTH during heating and cooling scans

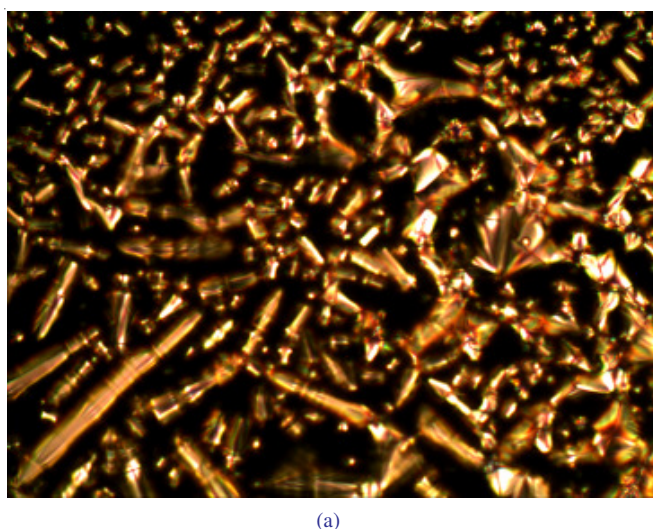
classical *schlieren* texture of nematic phase. However, in Fig. 3, upon cooling from isotropic liquid of 16MeBTH, emergence of SmA phase with *bâtonnets* texture can be observed. The presence of SmA phase was confirmed based on the microscopic observation of the characteristic fan shaped texture. All the observed liquid-crystalline textures were typical according to the literature^{10,11}.

It is well known that thermotropic liquid crystals are highly sensitive to their molecular constitution. The thermal stability and mesophase length as a measure of mesomorphism can be correlated with the molecular constitution of the compounds¹⁴.

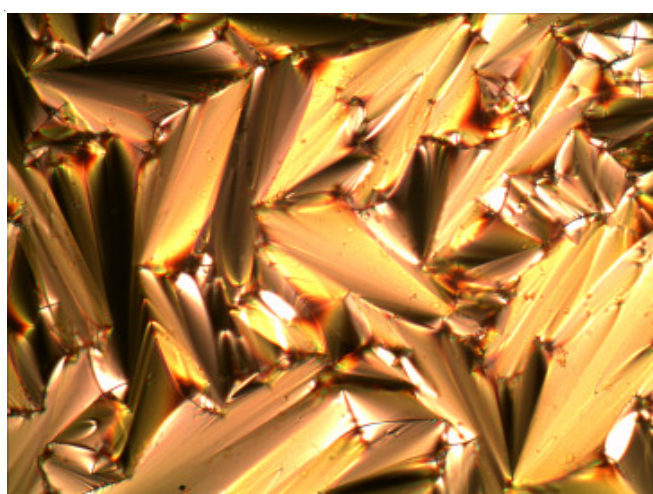
TABLE-1
PHASE TRANSITION TEMPERATURES AND ASSOCIATED ENTHALPY CHANGES OF SERIES nMeBTH

Compound	Cycle	Temperature (°C)	Phase transition	Associated enthalpy change (ΔH , kJ mol ⁻¹)
4MeBTH	Heating	99.6	Cr-to-N	31.02
		125.3	N-to-I	1.13
	Cooling	125.1	I-to-N	1.15
		63.8	N-to-Cr	26.38
6MeBTH	Heating	105.5	Cr-to-N	39.83
		119.5	N-to-I	1.03
	Cooling	119.4	I-to-N	1.47
		83.3	N-to-Cr	35.60
8MeBTH	Heating	108.2	Cr-to-N	49.10
		118.3	N-to-I	1.33
	Cooling	118.2	I-to-N	1.84
		96.2	N-to-SmA	1.43
10MeBTH	Heating	99.0	Cr-to-SmA	49.84
		110.7	SmA-to-N	3.41
		118.4	N-to-I	1.79
	Cooling	118.1	I-to-N	1.94
110.8		N-to-SmA	3.13	
12MeBTH	Heating	81.6	Cr-to-SmA	44.98
		116.1	SmA-to-I	8.25
	Cooling	116.7	I-to-SmA	8.90
		68.9	SmA-to-Cr	41.13
14MeBTH	Heating	83.2	Cr-to-SmA	48.79
		113.6	SmA-to-I	8.60
	Cooling	115.1	I-to-SmA	8.97
		69.7	SmA-to-Cr	47.86
16MeBTH	Heating	88.4	Cr-to-SmA	61.10
		115.8	SmA-to-I	10.45
	Cooling	115.5	I-to-SmA	10.94
		81.3	SmA-to-Cr	58.64
18MeBTH	Heating	55.6	Cr ₁ -to-Cr ₂	1.21
		91.2	Cr ₂ -to-SmA	67.18
		109.6	SmA-to-I	10.83
	Cooling	112.1	I-to-SmA	8.70
		86.6	SmA-to-Cr ₂	57.81
		54.7	Cr ₂ -to-Cr ₁	1.28

Note: Cr = crystal; I = isotropic; N = nematic; SmA = smectic A



(a)



(b)

Fig. 3. Optical photomicrographs of 16MeBTH on cooling. The battonnets (a) coalesced to form the fan-shaped texture of SmA phase in (b)

A plot of phase transition temperatures against the number of carbons in the alkoxy chains for series nMeBTH, enable the effects of the terminal chains on the mesomorphic properties to be studied (Fig. 4).

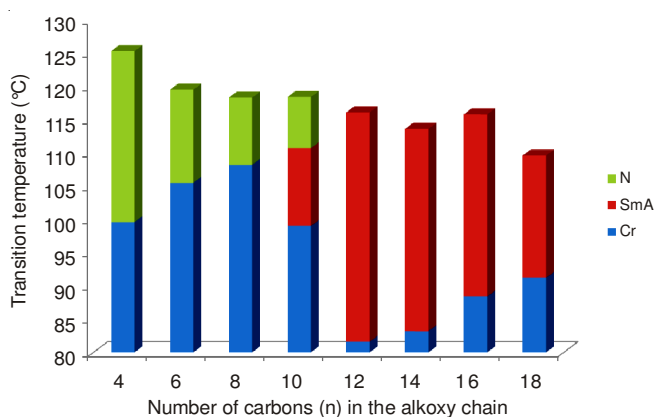


Fig. 4. Plot of transition temperature versus the number of carbon (n) in the alkoxy chain of nMeBTH

The present compounds exhibited liquid crystal properties where the terminal chain lengths are long enough for promoting

mesophase formation (nematic phase). Generally, compounds with short carbon chains exhibit wider nematic temperature ranges than compounds with longer alkoxy chains (Table-2)¹⁵. Smectogenic properties were observed as the chain length increased. In general, a metastable smectic phase commenced from C₈ member as monotropic phase and become a stable enantiotropic smectic phase from C₁₀ member and persistent till the end of the series. It can be clearly deduced that the length of the terminal chains can significantly affect the mesomorphic properties of the compounds¹⁶. The azomethine (C=N) linkage which conferred a step like structure resulted in the thickening effect which in turn enhanced the nematic phase for short to medium chain compounds⁷.

TABLE-2
MESOPHASE RANGE OF SERIES nMeBTH

Compound	Phase range, °C	
	Δ_{SmA}	Δ_N
4MeBTH	-	25.7
6MeBTH	-	14.0
8MeBTH	-	10.1
10MeBTH	11.7	7.7
12MeBTH	34.5 (widest)	-
14MeBTH	30.4	-
16MeBTH	27.4	-
18MeBTH	18.4	-

From the plot (Fig. 4), the clearing temperature showed descending trends as the length of the carbon chain increased. The flexible terminal alkoxy chain acts as a diluent to the mesogenic core rings system, hence, depressed the clearing temperature. The descending trend was in agreement with those series of 6-methoxy-2-(2-alkanoyloxybenzylideneamino)-benzothiazoles in which the homologous with the longest chain possessed the lowest thermal stability⁷. The increasing van der Waals forces resulted from the lengthening of alkyl chain that plays an important role in stabilizing the smectic phase by favouring the lamellar packing. On the other hand, it suppressed the nematic phase range¹⁷. In addition, the long carbon chain being attracted and intertwined which in turn facilitates the lamellar packing causing a reduction in the nematic phase range¹⁸. However, as the length of the carbon chain increase from C₁₀ to C₁₈ members, the smectic phase range (Δ_{SmA}) did not show a specific trend. Among all the smectogens, C12 member was found to possess the widest Δ_{mA} phase range (34.5 °C).

In order to confirm the presence of the smectic A phase in the series, XRD analysis was performed. The representative compound 16MeBTH is shown in Fig. 5. From XRD pattern of 16MeBTH, it has been revealed that the single sharp diffraction peak appeared at 1.605° indicating the presence of layered structure of smectic phase. It is well known that when the reflection within the SmA layer corresponds to d approximate to L, the SmA arrangement is in the monolayer form¹⁹. However, when the d-layer spacing is intermediate between L and 2L then it is called a partial bilayer phase¹⁴. According to XRD data, the d-layer spacing was found to be 37.9 Å. The layer spacing is much smaller than the molecular length and the d/L ratio was found to be 1.12. By combining the data from POM and XRD, SmA phase was identified to be present in compound 16MeBTH²⁰. It can be seen that the layer spacing

d, is significantly larger than the calculated molecular length (Table-3). This provides evidence for a partial bilayer structure of the smectic layers²¹.

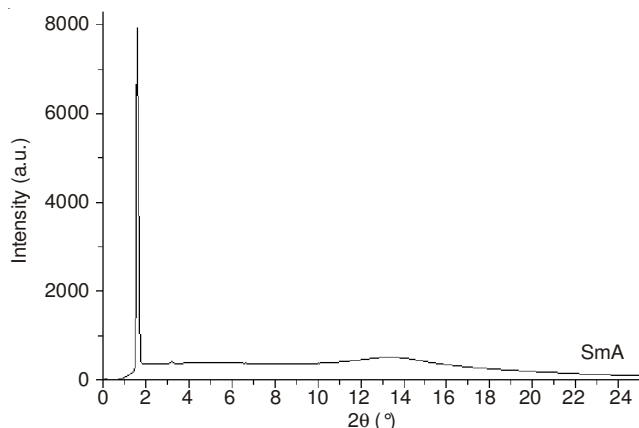


Fig. 5. X-ray diffraction patterns of 16MeBTH at different temperature on cooling from the isotropic phase

TABLE-3
POWDER X-RAY DIFFRACTION DATA OF 16MeBTH

Phase observed	SmA
Temperature (°C)	95 °C
2 theta (°)	1.605
d-spacing (Å)	37.9
Length, l (Å)	33.579
Aspect ratio (d/l)	1.12

ACKNOWLEDGEMENTS

The authors thank Ministry of Higher Education of Malaysia and Universiti Tunku Abdul Rahman for the financial supports and research facilities. The powder XRD measurements were supported by Beamline B117A (charged by Dr. Jey-Jau Lee) of the National Synchrotron Radiation Research Center, Taiwan.

REFERENCES

1. J.W. Goodby, V. Görtz, S.J. Cowling, G. Mackenzie, P. Martin, D. Plusquellec, T. Benvegnu, P. Boullanger, D. Lafont, Y. Queneau, S. Chambert and J. Fitremann, *Chem. Soc. Rev.*, **36**, 1971 (2007).
2. C.K. Lai, H.C. Liu, F.J. Li, K.L. Cheng and H.S. Sheu, *Liq. Cryst.*, **32**, 85 (2005).
3. A. Seed, *Chem. Soc. Rev.*, **36**, 2046 (2007).
4. S.T. Ha, T.M. Koh, S.T. Ong and Y. Sivasothy, *Chin. Chem. Lett.*, **20**, 1449 (2009).
5. A.K. Prajapati and N.L. Bonde, *Mol. Cryst. Liq. Cryst.*, **501**, 72 (2009).
6. A.I. Pavluchenko, N.I. Smirnova, V.V. Titov, E.I. Kovshev and K.M. Djumaev, *Mol. Cryst. Liq. Cryst.*, **37**, 35 (1976).
7. S.T. Ha, K.L. Foo, H.C. Lin, M.M. Ito, K. Abe, K. Kunbo and S.S. Sastry, *Chin. Chem. Lett.*, **23**, 761 (2012).
8. S.T. Ha, T.M. Koh, S.L. Lee, G.Y. Yeap, H.C. Lin and S.T. Ong, *Liq. Cryst.*, **37**, 547 (2010).
9. S.T. Ha, T.M. Koh, G.Y. Yeap, H.C. Lin, S.L. Lee, Y.F. Win and S.T. Ong, *Phase Transit.*, **83**, 195 (2010).
10. D. Demus and L. Ritcher, *Textures of Liquid Crystals*, Verlag Chemie, New York (1978).
11. L. Dierking, *Textures of Liquid Crystals*, Wiley-VCH, Weinheim (2003).
12. G.-Y. Yeap, T.-C. Hng, D. Takeuchi, K. Osakada, W.A.K. Mahmood and M.M. Ito, *Mol. Cryst. Liq. Cryst.*, **506**, 134 (2009).
13. S.-T. Ha, T.-M. Koh, H.-C. Lin, G.-Y. Yeap, Y.-F. Win, S.-T. Ong, Y. Sivasothy and L.-K. Ong, *Liq. Cryst.*, **36**, 917 (2009).
14. A.K. Prajapati and V. Modi, *Liq. Cryst.*, **37**, 1281 (2010).
15. K.C. Majumdar, S. Mondal, N. Pal and R.K. Sinha, *Tetrahedron Lett.*, **50**, 1992 (2009).
16. P.J. Collings and M. Hird, *Calamitic Liquid Crystals-Nematic and Smectic Mesophases*. In: *Introduction to Liquid Crystal Chemistry and Physics*, Taylor and Francis Ltd., London, pp. 43-77 (1997).
17. M.R. Fisch and S. Kumar, *Introduction of Liquid Crystals*, In: *Liquid Crystal: Experimental Study and Physical Properties and Phase Transition*, Cambridge University Press, United Kingdom, pp. 1-26 (2001).
18. G.Y. Yeap, S.T. Ha, P.L. Lim, P.L. Boey, M.M. Ito, S. Sanehisa and Y. Youhei, *Mol. Cryst. Liq. Cryst.*, **33**, 205 (2006).
19. C.C. Liao, C.S. Wang, H.S. Sheu and C.K. Lai, *Tetrahedron*, **64**, 7977 (2008).
20. H.S. Wang, Y.-J. Wang, H.-M. Hu, G.-H. Lee and C.K. Lai, *Tetrahedron*, **64**, 4939 (2008).
21. R.A. Reddy and B.K. Sadashiva, *J. Mater. Chem.*, **14**, 310 (2004).